Websites:
http://www.jofamericanscience.org
http://www.sciencepub.net

Emails:
editor@sciencepub.net
sciencepub@gmail.com

MARSLAND PRESS
Multidisciplinary Academic Journal Publisher

Multi-objective optimization of square beam subject to side impact for improvement of crashworthiness design

A. Farhaninejad [1], Rizal Zaharib [2], B.B. Sahari [1], Faieza Abdul Aziz [1], E. Rasooliyazdi [1]

[1.] Department of Mechanical and Manufacturing Engineering, Universiti Putra Malaysia, 43400 UPM Serdang, Selangor, Malaysia
[2.] Department of Aerospace Engineering, Faculty of Engineering, Universiti of Putra Malaysia, 43400 UPM Serdang, Selangor, Malaysia
alifarhaninejad@gmail.com

Abstract: Increasing energy absorption is a significant parameter in vehicle design. Absorbing more energy results in decreasing occupant damage. Limitation of the deflection in a side impact results in decreased energy absorption (SEA) and increased peakload (PL). Hence a high crash force jeopardizes passenger safety and vehicle integrity. The aims of this paper are to determine suitable dimensions and material and an appropriate reinforced structural design of a square beam subjected to side impact, in order to maximize SEA and minimize PL. To achieve this novel goal, the geometric parameters of a square beam are optimized using the response surface method (RSM). Both multi-objective and single-objective optimizations are performed, and the optimum design for different response features is obtained. A comparative analysis showing the relationship between these two parameters is presented.
[A. Farhaninejad, Rizal Zaharib, B.B. Sahari, Faieza Abdul Aziz, E. Rasooliyazdi. **Multi-objective optimization of square beam subject to side impact for improvement of crashworthiness design.** *J Am Sci* 2019;15(8):70-80]. ISSN 1545-1003 (print); ISSN 2375-7264 (online). http://www.jofamericanscience.org. 10. doi:10.7537/marsjas150819.10.

Keywords: crashworthiness, side impact, energy absorption, multi-objective optimization, square beam, SEA.

1. Introduction

Global accident statistics demonstrate that nearly 30% of accidents and 35% of fatalities are caused by side impact (Fildes et al., 2003, Dong et al., 2007). Side impact is more significant than frontal impact due to the reduced crash zone. Therefore there is a smaller crash zone to absorb energy in a side impact compared with the rear and front structure (Shilin et al., 2000, Strother, 1998). Hence there is no sufficient safety region when a passenger is completely subjected to impact, which results in severe injuries (Wang et al., 2006, Lee et al., 2008). Thus, increasing crash zones is essential but these may increase the weight of the vehicle. The crashworthiness performance of automobile components under crash conditions is very important for the vehicle occupants (Lee et al., 2008). On the other hand, the weight reduction of the vehicle is needed to improve fuel efficiency. Reducing the vehicle weight by about 10% results in a fuel saving of about 3-7% (Zhang et al., 2008).

For this reason thin-walled structures are increasingly used and a lot of research work has been carried out in past decades on the energy absorption of thin-walled structures under loading (Abramowicz and Wierzbicki, 1989, Kecman, 1983, Kim and Reid, 2001, Mamalis et al., 2006, Zhang et al., 2009, Wierzbicki and Abramowicz, 1983, Langseth and Hopperstad, 1996, Wierzbicki et al., 1994) . Kecman (Kecman, 1983) conducted experimental and theoretical analysis of the bending performance of rectangular beams.

In recent years, a lot of research work on vehicle crashes has been carried out. Cui (Cui et al., 2011) investigated lightweight multi-material components of automobiles with some new materials for enhancing crashworthiness. Niknejad (Niknejad et al., 2010) studied the fold creation in square columns under axial loading. Lee (Lee et al., 2008) investigated the energy absorption of thin-walled square tubes under impact loading. The effect of web corrugation under bending was investigated by C. L. Chan et al. (Chan et al., 2002). However, they have not considered the side impact on a square beam. Most of the research has analysed the axial crash of a square beam but neglected the lateral crash of a square beam, which is analysed in this research. Langseth et al. (Langseth et al., 1998, Langseth and Hopperstad, 1997) studied local buckling and the crush behaviour of square beams.

Many crash studies have been done considering rib structure (Marzbanrad et al., 2009, Zhang et al., 2009) but without an adequate focus on analysing the effects of different thicknesses of the structure and

applied ribs for improving crashworthiness. Finding the optimum point, considering maximum SEA and minimum PL with respect to their simultaneous limitation of deflection, is a major challenge. This optimum design point is critically important for vehicle components subjected to side impact. Meanwhile, a conflict between the criteria for these objectives is inevitable. This paper aims to present certain comparative steps and optimization methods to find the optimum point.

The modelling, meshing and crash analysis were done using the LS-DYNA suite of programs, and at a crash speed of 6 m/s. The thickness of the square beam is 1 mm. Figure 1 shows the dimensions of the structure and the condition of the impactor. This condition of square beam simulation could be a simplified representation of a front side sill door beam, as illustrated in Figure2. For this reason, in this research a side impact crash is considered.

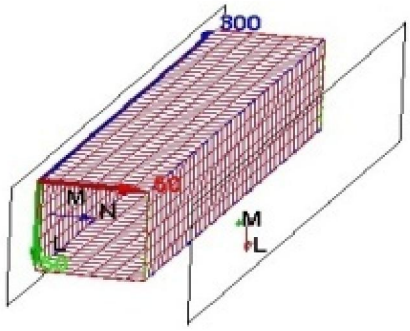

Fig. 1 View of moving rigid wall

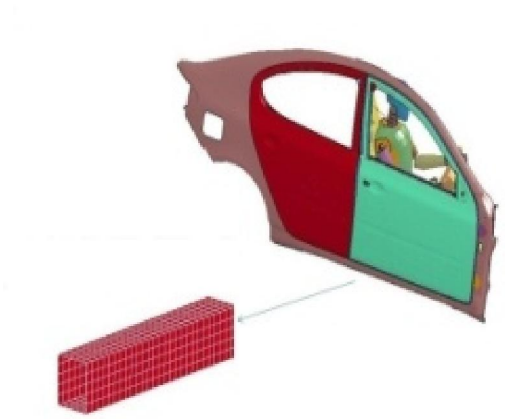

Fig. 2 Simplified beam of front side sill door

2. Methodology

2.1 Specific energy absorption

The energy E which is absorbed by the objects during the collision can be obtained from the following Equations:

$$E = \int_{v} A(\varepsilon) dv \quad (1)$$

where $A(\varepsilon)$ implies the total strain energy density of the corresponding structure. The specific energy absorption (SEA), which is the energy absorbed per unit mass of the structure part, can be defined by:

$$SEA = \frac{E_{total}}{M} \quad (2)$$

where E_{total} is the total energy and M is the mass of the corresponding structure under impact.

2.2 Finite element modeling

The CAD data of the square beam is modelled, meshed and simulated using LS-DYNA 3.1 Beta software from LSTC Co. In the analysis, the square beam is constrained with a rigid wall on one side, while the other side is impacted by a rigid wall of 10 kg mass moving with a constant velocity of 6 m/s. The four- node quadrilateral element (Belytschko-Tsay) is chosen because of its appropriate application in shell elements with the formulation of 3 integration points to mesh the model (Halquist, 2007).

2.3 Material properties

The properties of aluminium, steel and magnesium are assigned to the square beam. The mechanical properties of the materials are given in Table 1.

Table 1. Mechanical Properties of several materials

Material types	E (Gpa)	Poisson's Ratio	Yield stress (Mpa)	Ultimate stress (Mpa)	Strain at failure	Density (kg/m^3)
Aluminum 3105-H18	68.94	0.33	193	214	0.03	2720
Aluminum 201 -T3	70.3	0.35	296	379	0.15	2830
Steel AISI1006	200	0.3	190	320	0.3	7860

3. The effects of material on crashworthiness

Fig. 3 shows the lateral deflection for the square beam made of different materials. The maximum deflection occurs at 0.015 (s) for aluminium 3105 and at 0.01(s) for aluminium 2011 and steel, with deflections of 50 mm,43 mm and 34 mm for aluminium 3105, aluminium 2011 and steel respectively. The minimum deflection occurs to the steel due to its high rigidity compared with the aluminium alloys. Fig. 4 shows a comparison of the SEA for each material. It can be seen that the maximum SEA occurs with aluminium 2011, which is about 1.05162 (N.mm/ton). Thus, aluminium is a good choice due to its high SEA. However, the level of its deflection (43mm) is still high, which is analysed in the next step.

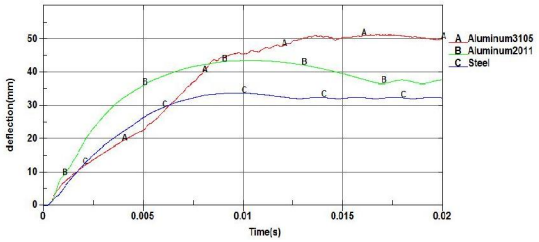

Fig. 3 Deflection for aluminium alloys and steel square beam

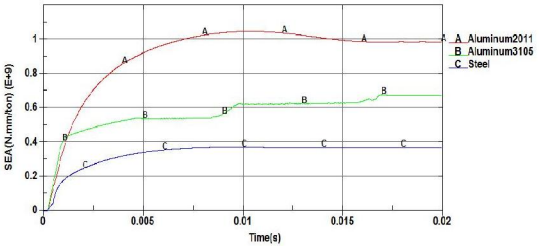

Fig. 4 SEA for aluminium alloys and steel beam square

4. The effects of reinforced structure on crashworthiness

In the previous step, it is observed that aluminium 2011 can be a good choice due to its high SEA. In this step, the limitation of deflection is considered. Fig. 5 shows the reinforced structure. The rectangular rib, with dimensions of $50 \times 300 \times 0.5$ mm, is placed horizontally in the middle lateral surface of the square beam structure with 1mm thickness. Fig. 6 shows the lateral deflection of the square beam made of aluminium 2011. It is observed that the level of deflection decreases from 43 mm for the simple structure to 3 mm for the reinforced structure. Therefore, the reinforced structure results in less deflection compared to the simple one. However, in Fig. 7 it is observed that the amount of SEA decreases from 1.05162 (E+9) (N.mm/ton) for the simple structure to 9.20052 (E+8) (N.mm/ton) for the reinforced structure. Thus, finding the optimum point which satisfies the maximum SEA and minimum peak load still remains a concern. Using optimization methods enables us to find this optimum design point.

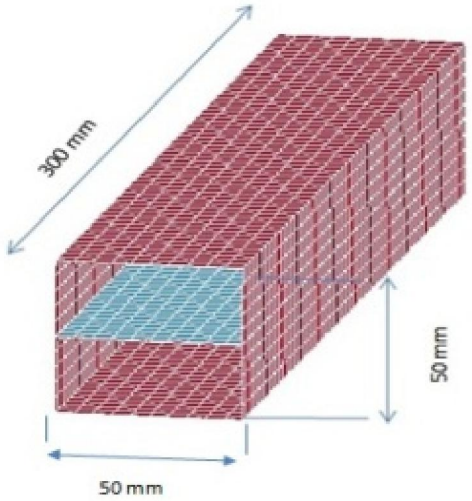

Fig. 5 Reinforced structure

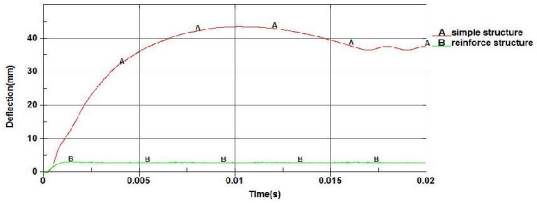

Fig. 6 Deflection of simple and reinforced structure

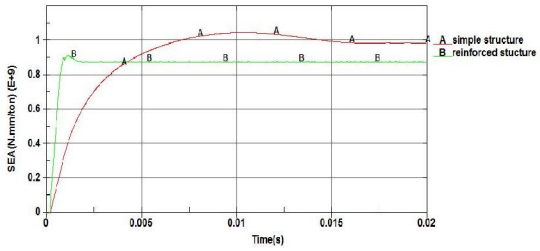

Fig. 7 SEA of simple and reinforced structure

5. Optimization problem

5.1Optimization problem description

Structural optimization techniques have been used recently for optimizing the energy absorption and peak load of structures under impact. There are a number of methods for optimization. The response surface method (RSM) is one of the methods most commonly used for crashworthiness optimization

(Salehghaffari et al., 2011, Hou et al., 2007, Acar and Rais-Rohani, 2009, Xiang et al., 2006). Yamazaki (Yamazaki and Han, 2000) , Lee (Lee and Lee, 2005) and Allahbakhsh (Allahbakhsh and Saemi, 2011) have applied an RSM method for crashworthiness optimization. In this paper, for optimizing specific energy absorption and peak load, both single-objective constrained and multi-objective optimization are applied. In the present paper, RSM as described by (Montgomery, 2008) is used and is described in this section. the results of changing geometry (thickness) is shown in Table 2.

Table 2. The results of SEA and PL

$t_s\ (mm)$	$t_r\ (mm)$	Mass (kg) ×10^-5	SEA (N.mm/tone) ×10^9	PL (N)
0.7	.2	12.69	1.24	83339
0.7	0.4	13.53	1.311	88120
0.7	0.5	13.95	1.269	90640
0.7	0.6	14.38	1.231	99643
0.73	0.2	13.19	1.304	88383
0.73	0.4	14.04	1.261	89933
0.73	0.5	14.46	1.225	97858
0.73	0.6	14.8	1.187	108129
0.75	0.2	13.53	1.278	88592
0.75	0.4	14.38	1.231	91813
0.75	0.5	14.8	1.193	101687
0.75	0.6	15.22	1.158	111317
0.8	0.2	14.38	1.137	97521
0.8	0.4	15.22	1.158	103958
0.8	0.5	15.65	1.126	110506
0.8	0.6	16.07	1.099	123574

The square beam is modeled with two different single-objective constrained problems. First is maximizing the SEA while PL is constrained. That is:

$$\begin{cases} Maximize \quad f_1 = SEA\ (x) \\ PL\ (x) \le PL_{const} \\ x^L \le x \le x^U \end{cases} \tag{3a}$$

where PL is the maximum peak load with the upper bound PL_{const}. In the second model, the optimum value of design variables is:

$$\begin{cases} Minimize \quad f_2 = PL_{\max}\ (x) \\ SEA\ (x) \ge SEA_{const} \\ x^L \le x \le x^U \end{cases} \tag{3b}$$

where SEA_{const} is the lower bound of SEA.

Multi-objective optimization can be formulated in two different ways, one of which is the linear weighted average as given in Equation (4):

$$\begin{cases} Minimize \quad F_w = (1-w)\dfrac{f_1^*}{f_1} + w\dfrac{f_2}{f_2^*} \\ \\ w \in [0,1]\ and \quad x^L \le x \le x^U \end{cases} \tag{4}$$

where f_1^*, f_2^* are the normalizing values of $f_1 = SEA(x)$ and $f_2 = PL(x)$ respectively (Fang et al., 2005, Zarei and Kröger, 2006, Hou et al., 2008) . w is the weight factor for emphasizing the different importance of each of the objectives (Athan and PANOS, 1996) .

Using the geometrical average of efficiency coefficients (Hou et al., 2009) with two objectives, another formulation is obtained for multi-objective optimization, as expressed in Equation (5):

$$\begin{cases} Maximize\ F_g = \sqrt{d_{SEA} d_p} \\ x^L \le x \le x^U \end{cases} \tag{5}$$

where d_{SEA} and d_p are efficiency coefficients of SEA and PL_{max} respectively. To maximize d_{SEA} in Equation (5), it is calculated in terms of the relative distance to the lower bound;

$$d_{SEA} = \frac{f_1(x) - f_1^L}{f_1^U - f_1^L} \tag{6}$$

and to minimize the peak crash force d_p is calculated as

$$d_p = 1 - \frac{f_2(x) - f_2^L}{f_2^U - f_2^L} \tag{7}$$

where f_2^U and f_2^L are the upper and lower bounds respectively. $f_1(x)$ and $f_2(x)$ are the functions of the design variables, and their values are in the interval [0,1]. When $F_g = 1$ the corresponding objective function reaches the optimal design, and if $F_g = 0$ it is the worst solution.

5.2 Response surface method

RSM is a method for illustrating the correlation between multiple variables as an input and an output. For the specific objective, functions like SEA and PL are assumed in terms of the basis function (Kurtaran et al., 2002, Yang et al., 2005, Myers et al., 1971) as:

$$\tilde{y}(x) = \sum_{j=1}^{N} a_j \varphi_j(x) \tag{8}$$

,

where N is the number of basis function $\varphi_i(x)$, $x \in R^n$. One type of basis function is polynomials, of which the quartic form is shown below:

$$\begin{aligned}
&\tilde{y} = a_0 + a_1 x_1 + a_2 x_2 + a_3 x_3 + \ldots && Linear\ terms \\
&a_{12} x_1 x_2 + a_{13} x_1 x_3 + a_{23} x_2 x_3 + \ldots && Interactio\ n\ terms \\
&a_{11} x_1^2 + a_{22} x_2^2 + a_{33} x_3^2 + \ldots && Quadratic\ terms \\
&\vdots \\
&a_{111} x_1^3 + a_{222} x_2^3 + a_{333} x_3^3 + \ldots && Cubic\ terms \\
&\vdots \\
&a_{1111} x_1^4 + a_{2222} x_2^4 + a_{3333} x_3^4 + \ldots && Quartic\ terms
\end{aligned} \tag{9}$$

To verify regression coefficient $a=(a_1,a_2,\ldots,a_N)$ in Equation (9), we need a large number for FE analysis $y^{(i)}(i=1,2,\ldots,M)\ (M\rangle N)$. By minimizing the errors between response function $\tilde{y}$ and FE analysis y, the regression coefficient vector a is determined. The least squares function is expressed in Equation (10)

$$E(a)=\sum_{i=1}^{M}\varepsilon_i^2=\sum_{i=1}^{M}[y^{(i)}-\sum_{j=1}^{N}a_j\varphi_j(x^{(i)})]^2 \tag{10}$$

and by $\dfrac{\partial E(a)}{\partial x}$ we can evaluate the regression coefficient vector $a=(a_1,a_2,\ldots,a_N)$, which is:

$$a=(\Phi^T\Phi)^{-1}(\Phi^T y) \tag{11}$$

Matrix Φ denotes the values of the basis functions that are evaluated for M sampling points as

$$\Phi=\begin{bmatrix}\varphi_1(x^{(1)}) & \cdots & \varphi_N(x^{(1)})\\ \vdots & \ddots & \vdots\\ \varphi_1(x^{(M)}) & \cdots & \varphi_N(x^{(M)})\end{bmatrix} \tag{12}$$

By substituting Equation (12) for Equation (8), the RS model can be defined.

5.3 Response surface model

In this paper the second order polynomial function is used for SEA (x) and PL (x) and these can be expressed as Equations (13) and (14) respectively.

$$\begin{aligned}SEA(t_s,t_r) &= -2.568\times10^{9}+1.127\times10^{10}t_s+6.221\times10^{8}t_r\\ &\quad -8.342\times10^{9}t_s^2-2.29\times10^{8}t_st_r-7.973\times10^{8}t_r^2\end{aligned} \tag{13}$$

$$\begin{aligned}PL(t_s,t_r) &= 2.187\times10^{5}-4\times10^{5}t_s-2.582\times10^{5}t_r\\ &\quad +3.205\times10^{5}t_s^2+2.378\times10^{5}t_st_r+1.673\times10^{5}t_r^2\end{aligned} \tag{14}$$

where t_s , t_r is structure and rib thickness respectively. The RS (response surface) of SEA and PL are shown in Figs. 8(a) and (b).

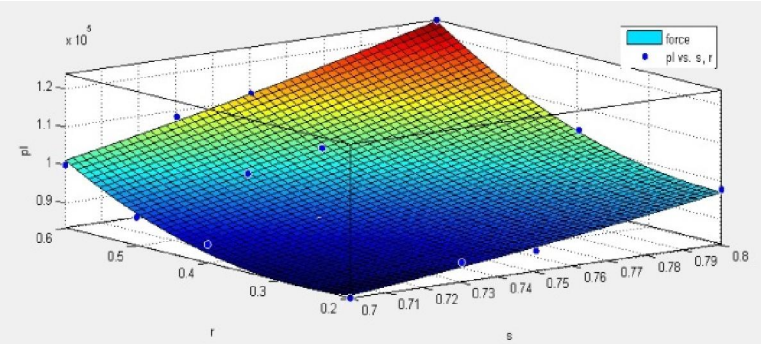

Fig. 8(a) Force surface fitting

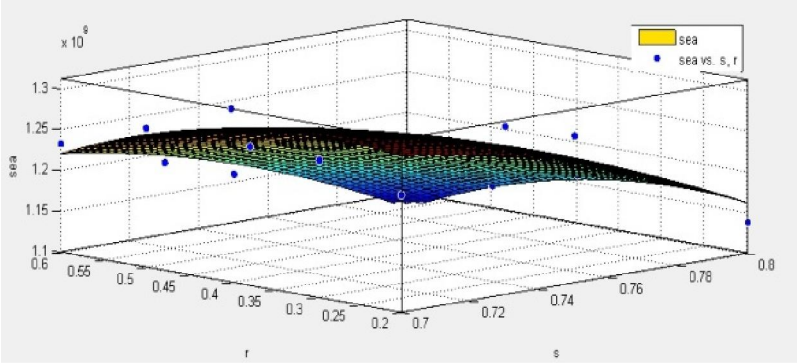

Fig. 8(b) SEA surface fitting

6. Design optimization results

6.1Constrained single-objective optimization

Two constrained single-objective optimization problems are defined for Equation (13) and Equation (14) as:

$$\begin{cases} Maximize & f_1 = SEA\,(r,t) \\ s.t & PL\,(r,t) \le 84\ KN \\ & 0.7 \le t_s \le 0.8 mm \\ & 0.2 \le t_r \le 0.6 mm \end{cases} \quad (15a)$$

and

$$\begin{cases} Minimize & f_2 = PL\ (r,t) \\ s.t & SEA\ (r,t) \ge 1.2 \times 10^9\ (N.mm\ /\ tone\ ) \\ & 0.7 \le t_s \le 0.8 \\ & 0.2\,mm \le t_r \le 0.6\,mm \end{cases} \quad (15b)$$

By applying a constrained non-linear multivariable optimization function in MATLAB, the optimum results of Equations (15a) and (15b) are obtained, as shown in Tables 3 and 4, respectively.

Table 3. The optimum result of Equation 15(a)

Optimal design variables (mm)	Max. SEA (N.mm/tone)
$t_s = 0.7, t_r = 0.29$	1.3003×10^9

Table 4. The optimum result of Equation 15(b)

Optimal design variables (mm)	Min.PL (N)
$t_s = 0.7, t_r = 0.27$	83171

6.2 Multi-objective optimization

In single-objective optimization, one criterion is investigated while the other one is constrained. So this method cannot explain the interaction between them. From a practical point of view, it seems that multi-objective optimization is more meaningful (Chen, 2005) . In this paper, SEA and PL are optimized by using the weighted average and geometrical average methods, respectively.

6.2.1The weighted average method

Multi-objective optimization accounts for the interaction between criteria (RAO, 1996) . Using the weighted average method, multi-objective optimization can be expressed as:

$$\begin{cases} Minimize & F(r,t) = (1-w)\dfrac{SEA^{*}}{SEA(r,t)} + w\dfrac{PL(r,t)}{PL^{*}} \\ & w \in [0,1] \\ & 0.7 \le t_s \le 0.8 \\ & 0.2\,mm \le t_r \le 0.6\,mm \end{cases} \tag{16}$$

where SEA^{*} and PL^{*} are the normalization values for SEA and PL respectively.

By varying weight w in Equation (16), the Pareto sets for the square beam are obtained as plotted in Fig. 9. The Pareto front provides a range of optimal solutions. The Pareto plot shows the relation between SEA and PL and any further improvement in SEA must sacrifice the PL and vice versa. In fact, any point in the Pareto frontier can be an optimal point, meaning that it is up to the designer to determine which factor is more important. For generating the Pareto frontier, the Genetic Algorithm (GA) multi-objective optimization solver of MATLAB is used.

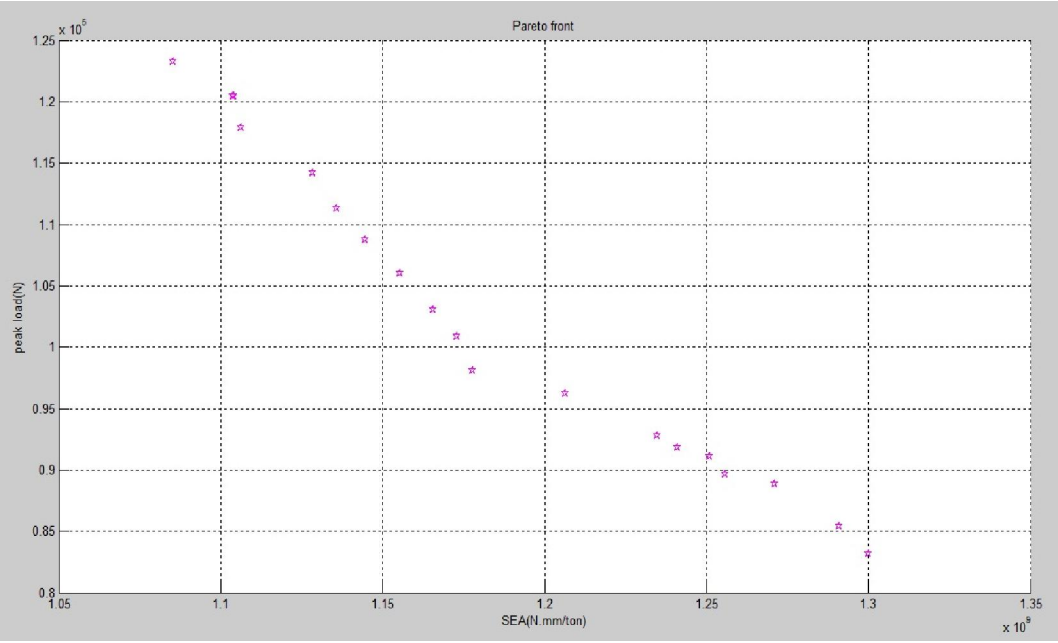

Fig. 9 Pareto graph

6.2.2 The geometrical average method

In this method, the cost function is constructed by the relative efficiency of two objectives. This is given as:

$$\begin{cases} Maximize & F_g(r,t) = \sqrt{d_{SEA} d_{PL}} \\ st & 0.7 \le t_s \le 0.8 \\ & 0.2 \le t_r \le 0.6 \end{cases} \tag{17}$$

$$d_{SEA} = \frac{SEA(r,t) - SEA^{L}}{SEA^{U} - SEA^{L}} \tag{18}$$

$$d_{PL} = 1 - \frac{PL(r,t) - PL^{L}}{PL^{U} - PL^{L}} \tag{19}$$

Where SEA^{U}, SEA^{L} and PL^{U}, PL^{L} represent maximum and minimum SEA and PL respectively. The results of maximizing the cost function $F_g(r,t)$ for the square beam are summarized in Table 5

Table 5. The result of cost function F_g

Optimal design variables (mm)	Cost function $F_g(r,t)$	SEA (N.mm/tone)	PL (N)
$t_s = 0.7$, $t_r = 0.27$	0.7	1.3002×10^9	83171

7. Discussion

In Table 3, it is observed that the optimum points which are obtained from the single-objective optimization and the geometrical average method are approximately the same. Comparing the finite element results and RS functions, it is proved that the RS method can be a good substitution in predicting the crashworthiness of a structure. On the other hand, the optimization method based on RS functions enables the expert to apply constrained objectives or algorithms to find a better design point. Utilizing these methods, allows the designer to analyse the effects of each independent variable of the responses (SEA, PL). However, finding a predominant objective from the list of design requirements is not easy, even for experts. For this reason, multi-objective optimization such as Pareto points enables the designer to have a group of solutions, unlike the single-objective method. It is observed that Pareto points generate a better design decision due to the various points based on SEA and PL.

8. Conclusion

From the results obtained and the discussion presented, the following conclusions are made:

1) Analysing the effect of material on crashworthiness leads to choose aluminium 2011 due to it's high SEA compared to steel and aluminium 3105.

2) The effects of reinforced structure on crashworthiness show that applying rib which located horizontally in the middle surface the square beam result in less deflection Limitation of deflection in a side impact leads to design a reinforced structure.

3) Increasing the amount of SEA for the aluminium 2011 reinforced structure result in using the optimization method. Maximizing SEA and minimizing PL are two important criteria in vehicle component design, which leads the designer to use a single-objective constrained method. The optimum points obtained from the constrained non-linear optimization algorithm lead us to a new understanding of the design point. Considering contrary objectives in the design simultaneously can be made possible by using non-linear constraint optimization algorithms.

4) Fitting the FEA results into the terms' basis function is a significant factor to give more attention to when substituting an RS approximation function in analysing crashworthiness. The RS function gives us the opportunity to predict the impact behaviour of a structure.

5) The multi-objective Pareto graph enables the designer to make a better decision on the design point. Having various optimum points based on two contrary objectives (SEA, PL) enables the designer to have a group of solutions to find the optimum point, which is considered to be the maximum SEA and minimum PL with respect to deflection.

References

1. ABRAMOWICZ, W. & WIERZBICKI, T. 1989. Axial crushing of multicorner sheet metal columns. *Journal of Applied Mechanics,* 56**,** 113.
2. ACAR, E. & RAIS-ROHANI, M. 2009. Ensemble of metamodels with optimized weight factors. *Structural and Multidisciplinary Optimization,* 37**,** 279-294.
3. ALLAHBAKHSH, H. & SAEMI, J. 2011. Design optimization of square and circular aluminium extrusion damage columns with crashworthiness criteria. *Indian Journal of Engineering & Materials Sciences,* 18**,** 341-350.
4. ATHAN, T. W. & PANOS, Y. P. 1996. A note on weighted criteria methods for compromise solutions in multi-objective optimization. *Engineering Optimization,* 27**,** 155-176.
5. CHAN, C., KHALID, Y., SAHARI, B. & HAMOUDA, A. 2002. Finite element analysis of corrugated web beams under bending. *Journal of Constructional Steel Research,* 58**,** 1391-1406.
6. CHEN, L. 2005. Mechanical optimization design methods. Beijing: Metallurgical Industry Press.
7. CUI, X., ZHANG, H., WANG, S., ZHANG, L. & KO, J. 2011. Design of lightweight multi-material automotive bodies using new material performance indices of thin-walled beams for the material selection with crashworthiness consideration. *Materials & Design,* 32**,** 815-821.
8. DONG, G., WANG, D., ZHANG, J. & HUANG, S. 2007. Side structure sensitivity to passenger car crashworthiness during pole side impact. *Tsinghua Science & Technology,* 12**,** 290-295.
9. FANG, H., RAIS-ROHANI, M., LIU, Z. & HORSTEMEYER, M. 2005. A comparative

study of metamodeling methods for multiobjective crashworthiness optimization. *Computers & structures,* 83**,** 2121-2136.
10. FILDES, B., BOSTROM, O., HALAND, Y. & SPARKE, L. Year. COUNTERMEASURES TO ADDRESS FARSIDE CRASHES: FIRST RESULTS. *In*, 2003.
11. HALQUIST, J. 2007. LS-DYNA keyword user's manual version 971. *Livermore Software Technology Corporation, Livermore, CA*.
12. HOU, S., LI, Q., LONG, S., YANG, X. & LI, W. 2007. Design optimization of regular hexagonal thin-walled columns with crashworthiness criteria. *Finite elements in analysis and design,* 43**,** 555-565.
13. HOU, S., LI, Q., LONG, S., YANG, X. & LI, W. 2008. Multiobjective optimization of multi-cell sections for the crashworthiness design. *International Journal of Impact Engineering,* 35**,** 1355-1367.
14. HOU, S., LI, Q., LONG, S., YANG, X. & LI, W. 2009. Crashworthiness design for foam filled thin-wall structures. *Materials & Design,* 30**,** 2024-2032.
15. KECMAN, D. 1983. Bending collapse of rectangular and square section tubes. *International Journal of Mechanical Sciences,* 25**,** 623-636.
16. KIM, T. & REID, S. 2001. Bending collapse of thin-walled rectangular section columns. *Computers & structures,* 79**,** 1897-1911.
17. KURTARAN, H., ESKANDARIAN, A., MARZOUGUI, D. & BEDEWI, N. 2002. Crashworthiness design optimization using successive response surface approximations. *Computational mechanics,* 29**,** 409-421.
18. LANGSETH, M. & HOPPERSTAD, O. 1996. Static and dynamic axial crushing of square thin-walled aluminium extrusions. *International Journal of Impact Engineering,* 18**,** 949-968.
19. LANGSETH, M. & HOPPERSTAD, O. 1997. Local buckling of square thin-walled aluminium extrusions. *Thin-walled structures,* 27**,** 117-126.
20. LANGSETH, M., HOPPERSTAD, O. & HANSSEN, A. 1998. Crash behaviour of thin-walled aluminium members. *Thin-walled structures,* 32**,** 127-150.
21. LEE, K. S., YANG, Y. J., KIM, S. K. & YANG, I. Y. 2008. Energy absorption control characteristics of AL thin-walled tubes under impact load. *Acta Mechanica Solida Sinica,* 21**,** 383-388.
22. LEE, T. H. & LEE, K. 2005. Multi-criteria shape optimization of a funnel in cathode ray tubes using a response surface model. *Structural and Multidisciplinary Optimization,* 29**,** 374-381.
23. MAMALIS, A., MANOLAKOS, D., IOANNIDIS, M. & KOSTAZOS, P. 2006. Bending of cylindrical steel tubes: numerical modelling. *International Journal of Crashworthiness,* 11**,** 37-47.
24. MARZBANRAD, J., ALIJANPOUR, M. & KIASAT, M. S. 2009. Design and analysis of an automotive bumper beam in low-speed frontal crashes. *Thin-walled structures,* 47**,** 902-911.
25. MONTGOMERY, D. C. 2008. *Design and analysis of experiments*, John Wiley & Sons Inc.
26. MYERS, R. H., MONTGOMERY, D. C. & ANDERSON-COOK, C. M. 1971. *Response surface methodology*, Allyn and Bacon Boston.
27. NIKNEJAD, A., LIAGHAT, G., NAEINI, H. M. & BEHRAVESH, A. 2010. Experimental and theoretical investigation of the first fold creation in thin walled columns. *Acta Mechanica Solida Sinica,* 23**,** 353-360.
28. RAO, S. S. 1996. Engineering optimization: theory and practice (3rd ed'96). *Recherche,* 67**,** 02.
29. SALEHGHAFFARI, S., RAIS-ROHANI, M. & NAJAFI, A. 2011. Analysis and optimization of externally stiffened crush tubes. *Thin-walled structures*.
30. SHILIN, H., JINHUAN, Z. & XIAODONG, W. 2000. Automobile Crash Safety. Beijing: Tsinghua University Press.
31. STROTHER, C. E. Year. Estimating vehicle deformation energy for vehicles struck in the side. *In*, 1998.
32. WANG, D., DONG, G., ZHANG, J. & HUANG, S. 2006. Car crashworthiness in pole side impact and MDB side impact. *Tsinghua Science & Technology,* 11**,** 725-730.
33. WIERZBICKI, T. & ABRAMOWICZ, W. 1983. On the crushing mechanics of thin-walled structures. *Journal of Applied Mechanics,* 50**,** 727.
34. WIERZBICKI, T., RECKE, L., ABRAMOWICZ, W., GHOLAMI, T. & HUANG, J. 1994. Stress profiles in thin-walled prismatic columns subjected to crush loading-II. Bending. *Computers & structures,* 51**,** 625-641.
35. XIANG, Y., WANG, Q., FAN, Z. & FANG, H. 2006. Optimal crashworthiness design of a spot-welded thin-walled hat section. *Finite elements in analysis and design,* 42**,** 846-855.
36. YAMAZAKI, K. & HAN, J. 2000. Maximization of the crushing energy absorption of cylindrical shells. *Advances in Engineering Software,* 31**,** 425-434.
37. YANG, R., WANG, N., THO, C., BOBINEAU, J. & WANG, B. 2005. Metamodeling development for vehicle frontal impact

simulation. *Journal of Mechanical Design,* 127**,** 1014.
38. ZAREI, H. & KRÖGER, M. 2006. Multiobjective crashworthiness optimization of circular aluminum tubes. *Thin-walled structures,* 44**,** 301-308.
39. ZHANG, X., JIN, X., LI, Y. & LI, G. 2008. Improved design of the main energy-absorbing automotive parts based on traffic accident analysis. *Materials & Design,* 29**,** 403-410.
40. ZHANG, Z., LIU, S. & TANG, Z. 2009. Design optimization of cross-sectional configuration of rib-reinforced thin-walled beam. *Thin-walled structures,* 47**,** 868-878.

8/18/2019